Broadband Determination of Microwave Permittivity and Loss in Tunable Dielectric Thin Film Materials[†]

James C. Booth, Leila R. Vale, and Ronald H. Ono*
*National Institute of Standards and Technology, 325 Broadway, Boulder, CO, 80303

ABSTRACT

We demonstrate a new method for determining the frequency-dependent dielectric properties of thin-film materials at microwave frequencies using coplanar waveguide (CPW) transmission line measurements. The technique makes use of the complex propagation constant determined from multiline thru-reflect-line (TRL) calibrations for CPW transmission lines to determine the distributed capacitance and conductance per unit length. By analyzing data from CPW transmission lines of different geometries, we are able to determine the complex permittivity of the dielectric thin film under study as a function of frequency from 1 to 40 GHz. By performing these measurements under an applied bias voltage, we are able in addition to determine the tuning and figure of merit that are of interest for voltage-tunable dielectric materials over the frequency range 1 to 26.5 GHz. We demonstrate this technique with measurements of the permittivity, loss tangent, tuning, and figure of merit for a 0.4 μm film of $Ba_{0.5}Sr_{0.5}TiO_3$ at room temperature.

INTRODUCTION

Voltage-tunable materials are technologically important for frequency-agile microwave applications, such as tunable filters[1], delay lines, and phase shifters[2]. The ability to electronically tune the frequency of operation of such devices, by changing the permittivity of a constituent material under an applied electric field, will enable many new high-performance microwave applications. In order to fabricate integrated devices, tunable materials in thin-film form are highly desirable. To date, however, thin-film materials that display the requisite tuning are hampered by very high microwave losses. In an effort to reduce the losses of tunable thin film materials, new candidate materials are being developed in ever increasing numbers. However, these materials are commonly evaluated for permittivity and loss at frequencies much lower than those required by the intended applications. Techniques at microwave frequencies that utilize well-characterized resonant cavity measurements are made difficult for these materials by the small volume occupied by films that are typically less than 1 μm in thickness. Characterization of these tunable materials at microwave frequencies is therefore made, if at all, using patterned thin-film devices, where the results often depend upon the specific device geometry used. While such measurements are adequate for optimizing a particular material system, they can be unsatisfactory for comparing different materials or for the subsequent design of devices that differ significantly from the test geometry used.

To address the need for measurements to characterize tunable thin-film materials at microwave frequencies, we have developed an experimental technique based on measurements of coplanar waveguide (CPW) transmission lines over the frequency range 0.1 to 40 GHz. We determine the loss and permittivity of dielectric thin films over this broad frequency range by analyzing the measured propagation constant for CPW transmission lines with and without the dielectric thin film under test. We make use of a distributed-circuit model (see Fig. 1) in order to determine the capacitance per unit length $C(\omega)$ and conductance per unit length $G(\omega)$ of the transmission lines incorporating the dielectric thin film from the measured propagation constants. We then analyze the distributed capacitance per unit length $C(\omega)$ and conductance per unit length $G(\omega)$ obtained by the use of different transmission-line geometries to extract geometry-independent quantities for the loss and permittivity of the dielectric film under test over the frequency range 0.1 to 40 GHz. Because these measurements can easily be performed in the CPW geometry under a

---

bias voltage (which is applied using standard bias tees), the change in permittivity with applied voltage, which defines the film tuning, can also be determined. The loss and tuning can in turn be used to obtain a single frequency-dependent figure of merit for the performance of the tunable dielectric thin film; the figure of merit is independent of specific device geometry.

These experimental determinations of the thin film loss and permittivity can be used to compare the performance of different materials, or to optimize the performance of a specific material. The coplanar waveguide geometry is particularly well suited for the planar devices that can be fabricated using epitaxial thin films on single-crystal substrates. The measurements described here are performed in a cryogenic microwave probe station at arbitrary temperatures from 350 K down to 20 K. Because the properties of interest of these tunable thin-film materials typically depend strongly on temperature, the cryogenic probe station is an ideal configuration for optimizing the microwave response of these materials. Knowledge of both the frequency dependence and the temperature dependence of the relevant dielectric properties can provide important physical clues to the origin of losses in these materials. Since the material properties extracted using this technique are independent of measurement geometry and span a broad frequency range, the results of these experiments can also be used by designers to predict the performance of devices incorporating these thin-film materials in any planar geometry at arbitrary frequency.

In what follows, we apply this new measurement technique to determine the dielectric properties of a 0.4 μm film of $Ba_{0.5}Sr_{0.5}TiO_3$ grown by pulsed laser deposition on a $LaAlO_3$ substrate. $Ba_{0.5}Sr_{0.5}TiO_3$ in thin-film form has been studied by a number of researchers for voltage-tunable applications[3-8]. We discuss in detail our determination of the propagation constant of our CPW transmission lines which are fabricated both on the dielectric thin film sample and on the bare substrate for a number of different CPW geometries. We also describe how we obtain the distributed circuit parameters ($C(\omega)$, $G(\omega)$) of the transmission lines, using two different analytical techniques. We then extract geometry-independent measures of loss, permittivity, tuning and figure-of-merit, as a function of frequency from 0.1 to 26.5 GHz. We conclude with a discussion of the errors and limitations of this technique for determining loss, permittivity, and tuning of dielectric thin-film materials.

EXPERIMENT

Capacitance and Conductance in Coplanar Waveguide Transmission Lines

We obtain the complex propagation constant $\gamma = \alpha + i\beta$, where α is the attenuation constant and β is the phase constant, of our CPW transmission lines as a function of frequency by performing a multiline thru-reflect-line (TRL) calibration[9]. The TRL calibration uses planar CPW calibration sets consisting of individual elements that are all fabricated using the same geometry (center conductor linewidth, gap spacing, metalization thickness, etc., see Fig. 1(b)). An individual calibration set consists of a thru (defined as a transmission line of zero length), a short-circuit reflect, and transmission lines of different lengths. For the measurements described here, we fabricate the CPW devices using silver films 0.5 to 1 μm thick for the metallic conductors, with a center conductor linewidth (2s in Fig. 1(b)) of 55 μm. We fabricate three distinct calibration sets which have gap spacings (g in Fig. 1(b)) of 100 μm, 50 μm, and 25 μm. By measuring the S-
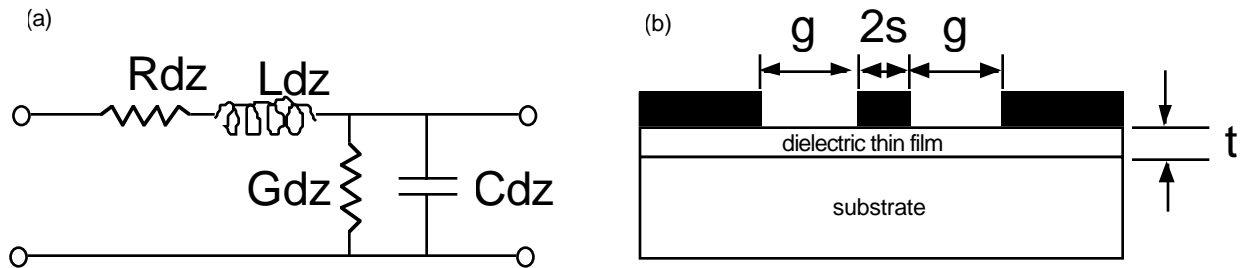

Fig. 1. Schematic diagram showing (a) distributed-circuit model for a transmission line, and (b) CPW cross-section. R, L, C, G are the resistance, inductance, capacitance, and conductance per unit length.

parameters of the individual devices in each calibration set using movable air coplanar probes, we are able to obtain the complex propagation constant of the CPW transmission lines in that particular calibration set using the Multical algorithm developed at NIST [9]. Figure 2 shows the measured attenuation and relative phase constant obtained in this manner for the 50 μm gap calibration set fabricated on a bare $LaAlO_3$ substrate, and on a substrate onto which a 0.4 μm film of $Ba_{0.5}Sr_{0.5}TiO_3$ had been deposited. The increase in both the attenuation and phase constant due to the $Ba_{0.5}Sr_{0.5}TiO_3$ thin film is substantial. Also shown in Fig. 2 is the effect of a bias voltage of 50 V on the propagation constant. For these measurements, the bias tees that we use limit the frequency range to 0.1 to 26.5 GHz.

Once we have obtained the propagation constant for both the test (dielectric film and substrate) and the reference (bare substrate only) transmission lines, we use two different techniques to extract the capacitance and conductance per unit length of the transmission lines on the dielectric thin film under study. The first technique, called the calibration comparison technique[10], uses a comparison of the TRL calibrations of the test and reference calibration sets
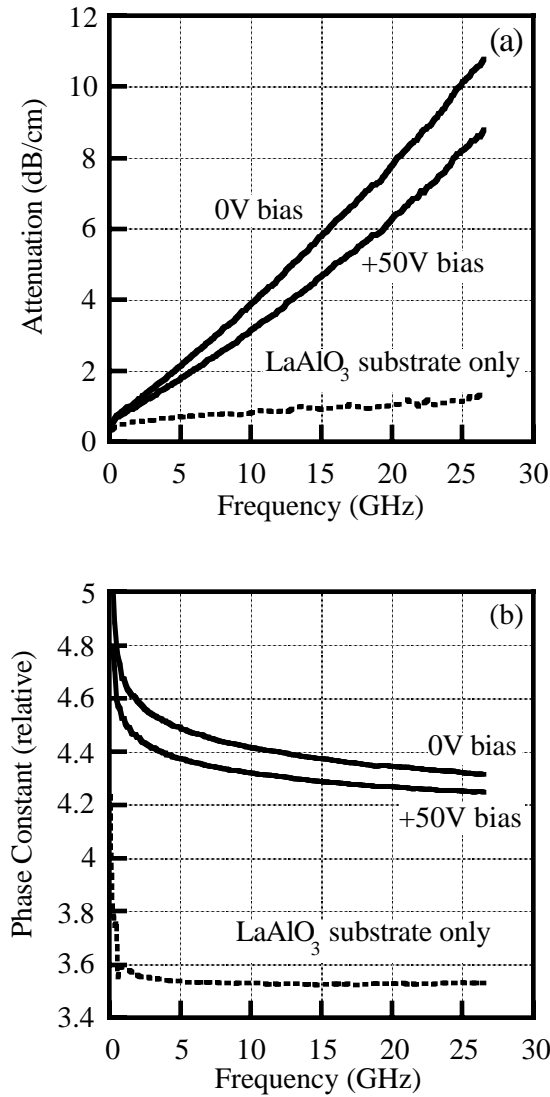

Fig. 2. Measured values at room temperature for the (a) attenuation constant and (b) relative phase constant for CPW transmission lines on a bare $LaAlO_3$ substrate on a $LaAlO_3$ substrate onto which a 0.4 μm film of $Ba_{0.5}Sr_{0.5}TiO_3$ has been deposited. The CPW metalization is silver 0.5 μm thick with a center conductor linewidth of 55 μm and a gap spacing of 50 μm. Also shown are values for the attenuation and relative phase constant under the application of a dc bias voltage of 50V.

with a TRL calibration on a third sample that has been well characterized. The third sample consists of gold lines on a quartz substrate. These lines are fabricated with embedded lumped resistors that are used to determine the capacitance per unit length[11] and hence the characteristic impedance[12] of the quartz calibration sets. We use the calibration comparison technique to obtain the (complex) characteristic impedance Z_0 of the lines on our test and reference samples. We then combine the characteristic impedance with our measured values of the propagation constant γ to obtain the distributed circuit parameters R, L, C, and G vs. frequency[13] for the both the test and reference samples:

$$\frac{\gamma}{Z_0} = G + i\omega C$$

$$\gamma Z_0 = R + i\omega L \quad ,$$

(1)

where R and L are the distributed resistance and inductance per unit length, while C and G are the distributed capacitance and conductance per unit length. We then assume that the contribution to the capacitance and conductance due to the dielectric film is given by the difference between the capacitance and conductance of the test and reference samples.

We also determine the capacitance and conductance per unit length $C(\omega)$ and $G(\omega)$ of the CPW transmission lines fabricated on the dielectric thin film under study using the equivalent-impedance method described by Janezic and Williams[14]. This method makes use of the fact that the ratio of the propagation constant of the lines on the test sample (incorporating the dielectric thin film) to the propagation constant of the lines on the reference sample (bare substrate) is given by the following:

$$\frac{\gamma_t}{\gamma_r} = \sqrt{\frac{(R_t + i\omega L_t)(G_t + i\omega C_t)}{(R_r + i\omega L_r)(G_r + i\omega C_r)}} \quad ,$$

(2)

where R, L, C, and G are the distributed circuit parameters of the test lines (film and substrate, subscript t) and the reference lines (substrate only, subscript r) respectively. Since we expect the loss tangent of LaAlO$_3$ to be approximately 10^{-4} or smaller, we assume that the conductance per unit length of the bare substrate is negligible, so that we can ignore G_r in Eq. (2). We assume that the inductance and resistance per unit length are identical for the test and reference samples ($R_t = R_r$, $L_t = L_r$). In order to realize this experimentally, we fabricate the metallic lines on the bare substrate and dielectric sample simultaneously in the same deposition system. We will present below experimental evidence that this assumption ($R_t = R_r$, $L_t = L_r$) is valid for the calibration sets described here. With these assumptions, we can obtain the conductance and capacitance per unit length of the test sample as long as the capacitance per unit length of the reference lines is known:

$$G_t + i\omega C_t = i\omega C_r \left(\frac{\gamma_t}{\gamma_r}\right)^2 .$$

(3)

To obtain $C_r(\omega)$ in Eq. (3) above, we use results from the calibration comparison technique described previously. Figure 3 shows the capacitance per unit length for CPW lines on a bare LaAlO$_3$ substrate determined by the calibration comparison method. Also shown in this figure is the capacitance per unit length that is calculated for the geometry under consideration by use of a finite element analysis with a relative permittivity of 23.2 for the LaAlO$_3$ substrate. The finite element model uses three dimensional conductors that are perfect conductors, and the results for $C(\omega)$ show a frequency dependence that is similar to that obtained using the calibration comparison technique. We use a quadratic fit to $C_r(\omega)$ for the lines on the bare substrate in the equivalent-impedance method, Eq. (3), to determine $C_t(\omega)$ and $G_t(\omega)$ for the lines incorporating the dielectric thin film.

We also use the calibration-comparison technique to obtain the resistance and inductance per unit length for the lines on the bare substrate (reference sample) as well as for the lines incorporating the dielectric thin film (test sample), to determine if they are indeed equivalent, as required by the equivalent-impedance method. Such a comparison is shown in Fig. 4. From this figure it is clear that the assumptions are in fact valid for the sample considered here.
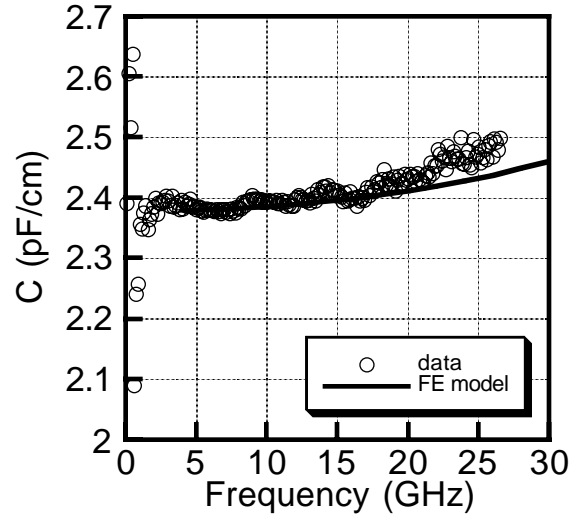
Fig. 3. The measured capacitance per unit length vs. frequency for CPW transmission lines on a bare LaAlO$_3$ substrate at room temperature. The CPW metalization is silver 0.5 μm thick with a center conductor linewidth of 55 μm and a gap spacing of 100 μm. The solid line is the result of a finite element calculation for the same geometry using a relative dielectric constant of 23.2 for LaAlO$_3$.

We can now use the determination of $C_r(\omega)$ in Fig. 3 to calculate $C_t(\omega)$ and $G_t(\omega)$ for the lines on the dielectric film under test using the equivalent-impedance method Eq. (3). The results are illustrated in Fig. 5, which shows the capacitance per unit length $C_t(\omega)$ and the device loss tangent $G_t(\omega)/\omega C_t(\omega)$ determined using the equivalent-impedance technique as well as the calibration comparison technique. This figure shows that both techniques yield similar values for $C_t(\omega)$ and $G_t(\omega)/\omega C_t(\omega)$, although the two different techniques make use of very different assumptions. The equivalent impedance method gives less scatter in the determination of $C_t(\omega)$ and $G_t(\omega)/\omega C_t(\omega)$.

Once we have determined the device capacitance per unit length, we obtain the contribution that is due to the dielectric film by simply subtracting the substrate capacitance per unit length from the total device capacitance per unit length. This is equivalent to assuming that the capacitance due to the dielectric film adds in parallel to that of the substrate and air to give the total capacitance. We also assume that the device conductance is due entirely to the dielectric film. We determine $C_{film}(\omega)$ and $G_{film}(\omega)$ for calibration sets having different gap spacings, which are shown in Fig. 6. As expected, as the gap spacing decreases both the capacitance and conductance per unit length increase. Note that the $G_t(\omega)/\omega C_t(\omega)$ in Fig. 6 is the loss tangent of the entire device, which can be related to the loss tangent of the dielectric thin film approximately by

$$\tan \delta_{film} \approx \frac{G_t(\omega)}{\omega C_t(\omega)} \frac{C_t(\omega)}{C_{film}(\omega)} \qquad . \tag{4}$$

Permittivity and Loss Tangent Determination

In order to obtain the complex permittivity as a function of frequency, we need an expression that relates ε' and ε'' to C_{film} and G_{film}, respectively. One can use a conformal mapping approach[15] to obtain an analytical expression for the contribution to the capacitance due to a thin film in the CPW geometry:

$$C_{film} = \varepsilon_0 \left(\varepsilon_r - \varepsilon_{sub} \right) \frac{K(k)}{K(k')}$$

$$k = \frac{\sinh(\pi s/2t)}{\sinh(\pi (s+g)/2t)} \qquad . \tag{5}$$
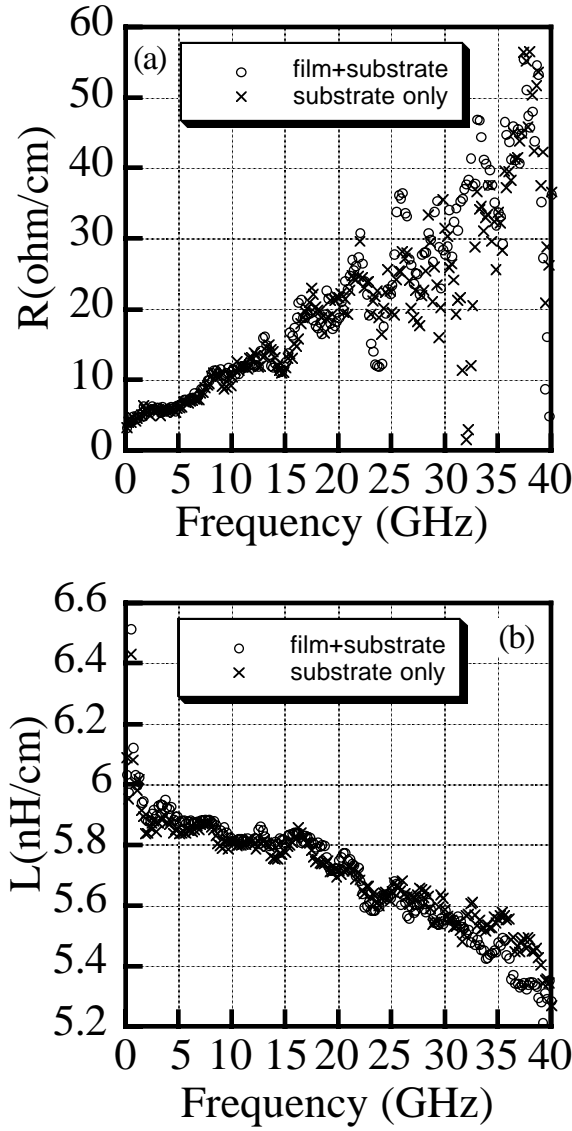
5

Fig. 4. Measured values for the (a) resistance per unit length and (b) inductance per unit length vs. frequency for a CPW transmission line with and without a 0.4 μm film of $Ba_{0.5}Sr_{0.5}TiO_3$. The CPW metalization is silver 0.5 μm thick with a center conductor linewidth of 55 μm and a gap spacing of 100 μm. The substrate is $LaAlO_3$.

In Eq. (5) ε_r is the relative permittivity of the film, ε_{sub} is the relative permittivity of the substrate, 2s is the center conductor linewidth, g is the gap spacing, and t is the film thickness (see Fig. 1(b)). Here K is the complete elliptic integral of the first kind, and $k' = (1-k^2)^{1/2}$. For the case of thin films $(t << s, g)$, this expressions simplifies to

$$C_{film} \approx \varepsilon_0 (\varepsilon_r - \varepsilon_{sub}) \frac{2t}{g} \qquad (t << s, g) \quad . \qquad (6)$$

If we now plot the measured film capacitance (per unit length) at a fixed frequency as a function of t/g, we can extract the permittivity from the slope of the resulting straight line. This is illustrated in Fig. 7, which shows that the film capacitance at 10 GHz is indeed linear in t/g, for dimensions such that t/g < 0.01. We obtain the real part of the permittivity at this frequency from the slope of C_{film} vs. t/g, and obtain the imaginary part of the permittivity from the slope of G_{film}/ω vs. t/g. Note from Fig. 7 that both quantities C_{film} and G_{film}/ω have finite intercepts as t/g approaches zero. This feature is not predicted by the conformal mapping expression Eq.(6), which predicts that C_{film} and G_{film}/ω approach zero as t/g approaches zero.

In order to gain further insight into the behavior of C_{film} and G_{film}/ω as a function of CPW geometry, we have performed a number of finite element simulations for the geometries discussed
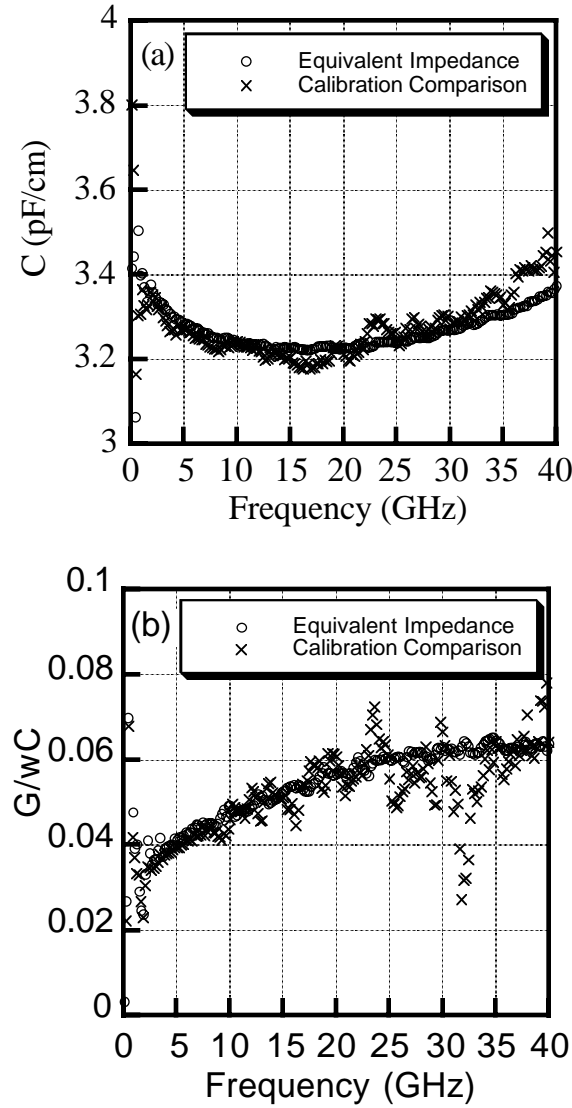
Fig. 5. Measured values using two different techniques of (a) the capacitance per unit length and (b) device loss tangent vs. frequency for CPW transmission lines fabricated on a 0.4 µm film of $Ba_{0.5}Sr_{0.5}TiO_3$. The CPW metalization is silver 0.5 µm thick with a center conductor linewidth of 55 µm and a gap spacing of 100 µm. The substrate is $LaAlO_3$.

here using a commercially available software package. We extract the film capacitance and conductance per unit length using the equivalent impedance analysis of the numerically calculated propagation constants. Analysis of such data yields plots very similar to Fig. 7, which have a finite intercept in plots of C_{film} and G_{film}/ω vs. t/g. This analysis of the simulated data gives values for the permittivity correct to within about 1 %, suggesting that the analytical technique presented here has reasonable accuracy.

We can now extract values for the real and imaginary parts of the permittivity as a function of frequency by performing the linear fits described above at each frequency point for the data shown in Fig. 6. We plot the results as $e_r'(\omega)$ and as loss tangent $\tan\delta(\omega)$ in Fig. 8 for the $Ba_{0.5}Sr_{0.5}TiO_3$ film at room temperature. Note from Fig. 8 the considerable frequency dependence observed in both $e_r'(\omega)$ and $\tan\delta(\omega)$ over the range 1-26.5 GHz.
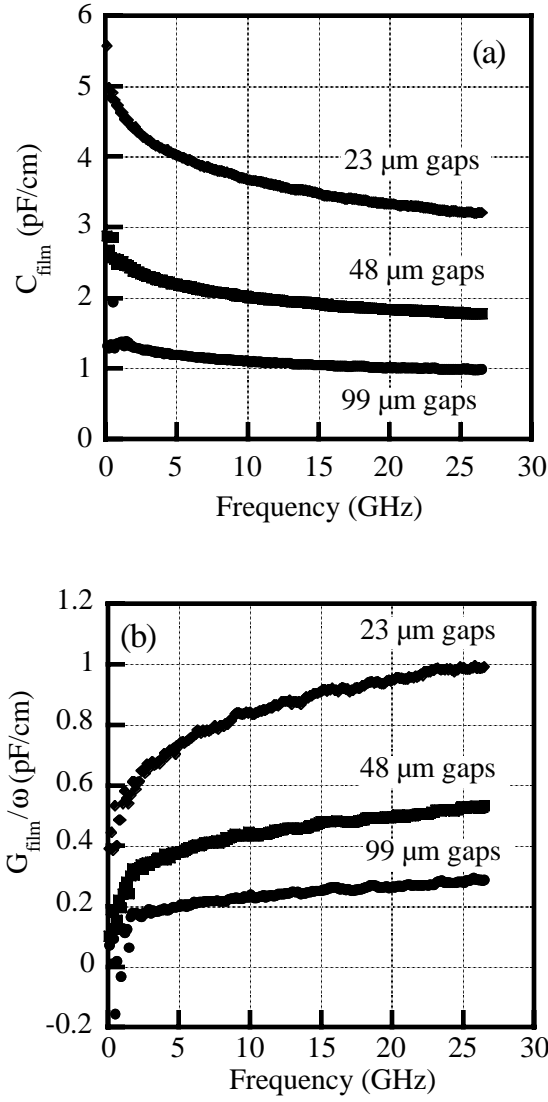
Fig. 6. Measured values for three different CPW geometries at room temperature of (a) the film capacitance per unit length and (b) film conductance per unit length vs. frequency for lines fabricated on a 0.4 μm film of $Ba_{0.5}Sr_{0.5}TiO_3$. The CPW metalization is silver 0.5 μm thick with a center conductor linewidth of 55 μm. The substrate is $LaAlO_3$.

Tuning And Figure of Merit Determination

For materials such as $Ba_{0.5}Sr_{0.5}TiO_3$ the quantities of technological interest are the loss tangent and the amount of tuning that can be achieved for a given bias voltage. We can determine the tuning by simply measuring the change in the capacitance per unit length for a given applied bias voltage. We then define the relative tuning T as:

$$T(V) = \frac{\varepsilon_r(0) - \varepsilon_r(V)}{\varepsilon_r(0)} = \frac{\left[C_{film}(0) - C_{film}(V)\right]}{\varepsilon_r(0) \cdot 2\varepsilon_0 t/g} \quad , \tag{7}$$

where we have used Eq. (6) to relate the change in ε_r to the change in C_{film} so that Eq. (7) is valid only in the thin film limit (t << s, g). Note that the tuning for a particular film depends on the applied bias voltage, so that the value specified for the tuning is meaningful only if a corresponding bias voltage (or field) is specified. An example of the tuning measured for a $Ba_{0.5}Sr_{0.5}TiO_3$ thin film at room temperature for a bias field of 2 V/μm is shown in Fig. 9(a) (we assume that the average bias field E_{bias} in the film is related to the applied voltage V and gap spacing as $E_{bias} = V/g$).
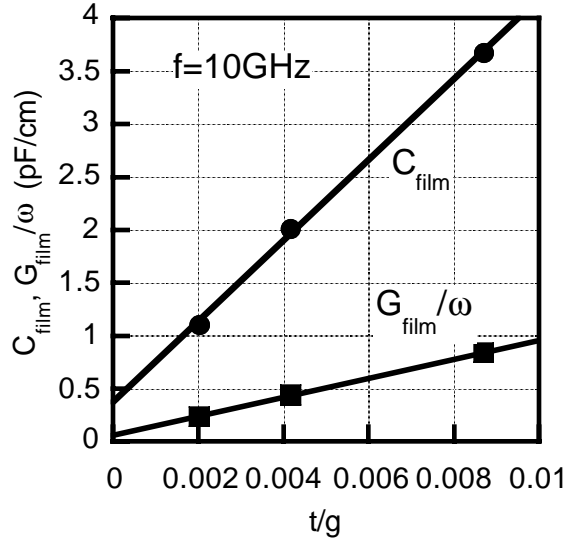
8

Fig. 7. Measured capacitance and conductance per unit length as a function of t/g at a measurement frequency of 10 GHz. The CPW metalization is silver 0.5 μm thick with a center conductor linewidth of 55 μm. The substrate is $LaAlO_3$.

Defined in this manner, the tuning divided by 2 gives the relative change in frequency or phase achievable for a tunable filter or phase shifter. Note that this definition is independent of the film thickness used. The film thickness and specific geometry must be used, however, to calculate the tuning of any actual device.

In order to compare the performance of different tunable dielectric materials, measured perhaps at different temperatures, it is convenient to define a figure of merit that takes into account the tuning and loss of a thin film material, since it is quite common for materials that have a large tuning factor to also have high losses. We use the following definition for a figure of merit K(V):

$$K(V) = \frac{T(V)}{\tan \delta_{max}} \quad (8)$$

The higher the value for K(V) for a given applied voltage, the better the performance of the material. We show in Fig. 9(b) the figure of merit at room temperature for a $Ba_{0.5}Sr_{0.5}TiO_3$ thin film. Although this material exhibits considerable tuning (see Fig. 9(a)), the high loss tangent results in a K(V) value at $E_{bias} = 2$ V/μm of order unity over most of the frequency range. Also note from Fig. 9(b) that the figure of merit drops by a factor of 2 from 5 GHz to 25 GHz.

Measurement Errors and Resolution

The sensitivity of this measurement technique can be defined as the smallest value for the loss tangent, or the smallest change in capacitance that can be extracted from the measured quantities. Examination of Eq. (3) shows that errors in G_t and C_t result directly from errors in the experimental determination of C_r and the relevant propagation constants. Additional errors come from the extraction of C_{film} from C_t. In the determination of the permittivity, additional errors come from uncertainties in the CPW dimensions t and g. Note, however, the loss tangent and tuning determinations (and hence also the figure of merit determination), are independent of the film thickness and CPW dimensions (and associated errors).

In order to estimate some of these uncertainties, it is necessary to determine the reproducibility errors associated with the propagation constant measurements. This is easily accomplished by using the calibration comparison technique[10] which was introduced previously for determining the characteristic impedance of a given calibration set. By using this technique to compare two calibrations performed on the same calibration set, it is possible to determine the upper bound for errors in measured S-parameters for a given calibration. By relating the errors in S-parameters to errors in the propagation constant, we are able to place a limit on the smallest measurable loss tangent and tunability for a given calibration set. We find that the resolution of the
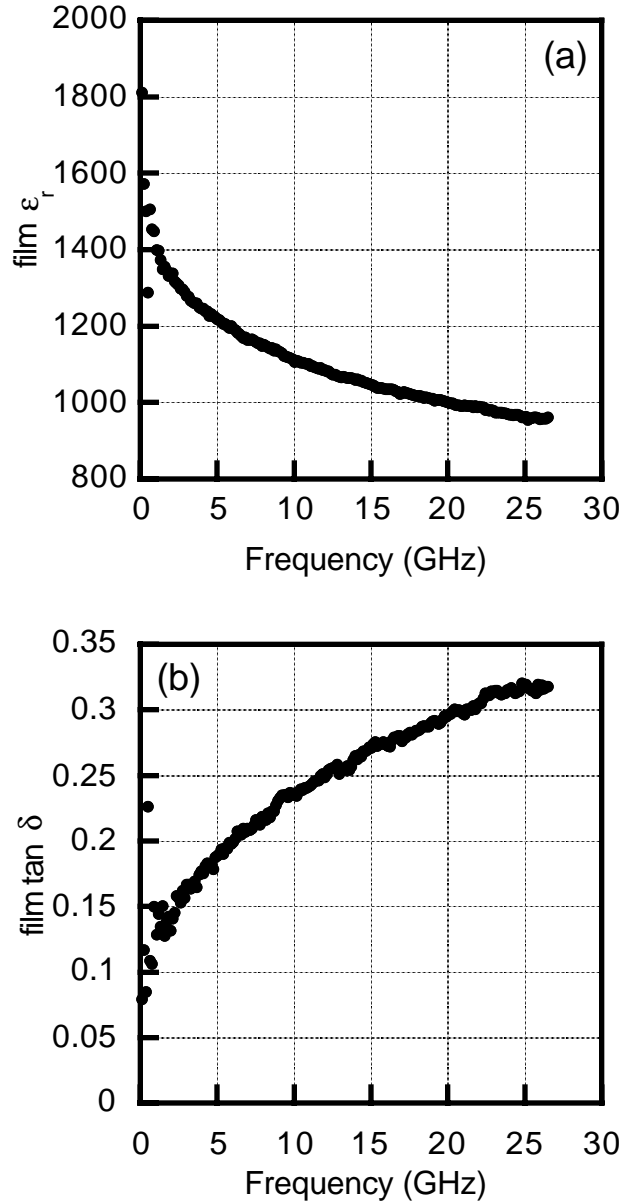
9

Fig. 8. Measured values for the (a) film relative permittivity and (b) film loss tangent as a function of frequency for a 0.4 μm film of $Ba_{0.5}Sr_{0.5}TiO_3$ at room temperature.

measurement for $\tan\delta_{film}$ and $\Delta C/C_{film}$ is proportional to the repeatability errors discussed above, and inversely proportional to the filling factor of the dielectric as well as the absolute phase of the transmission line. This means that we obtain better resolution for higher dielectric constants, higher frequencies, and longer transmission lines. For the geometries considered here, the smallest resolution we can achieve is on the order of 0.01 for both $\Delta C/C$ and $\tan\delta$, for frequencies greater than about 5 GHz.

The resolution quoted above is the best one can achieve using this technique if all other quantities are known exactly. In practice the determination of the errors involved in the measurement of $C_r(\omega)$ are much more difficult to quantify than errors in the propagation constant. We do note that our determination of C_r agrees reasonably well with simulation results for a reasonable value for the substrate relative permittivity ($\varepsilon_{sub} \sim 23.3$), see Fig. 3. For the permittivity determinations, errors in t and g are on the order of 5-10 % and most likely dominate the other sources of error. As mentioned previously, these errors do not affect the determination of $\tan\delta$, tuning, or figure of merit.
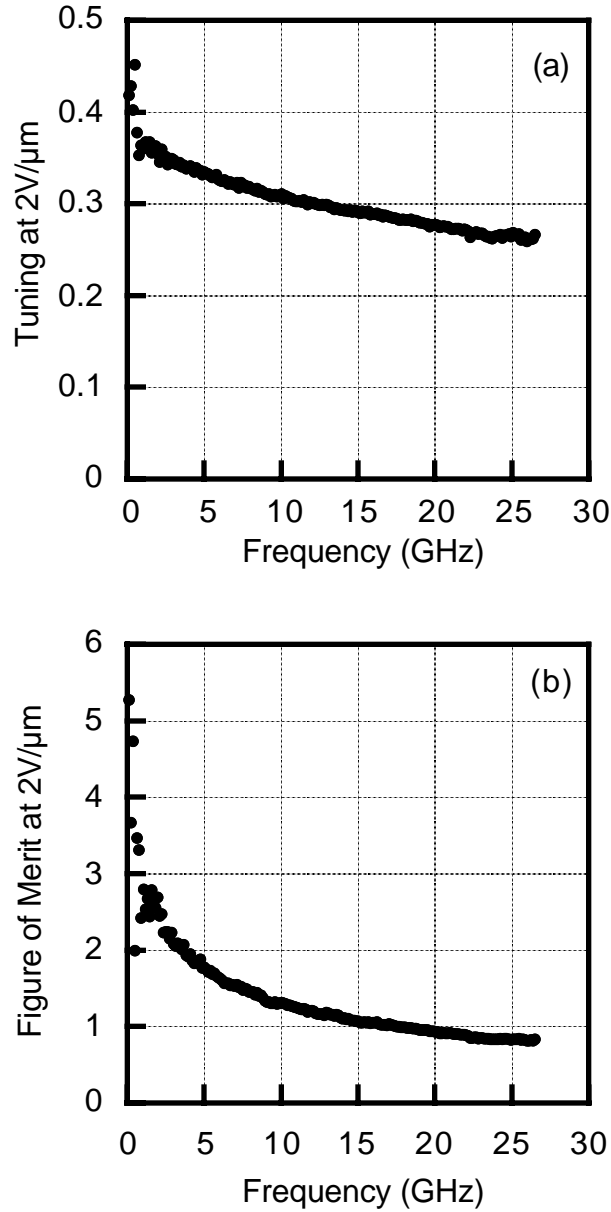
Fig. 9. Measured values for the (a) film tuning and (b) film figure of merit as a function of frequency at a bias field of 2 V/µm for a 0.4 µm film of $Ba_{0.5}Sr_{0.5}TiO_3$ at room temperature. The tuning and figure-of-merit are determined from $\Delta C_{film}(V)$ of the 25 µm gap calibration set.

CONCLUSIONS

We have demonstrated an experimental technique based on CPW transmission line measurements for the determination of the dielectric properties of thin film materials. Using multiline TRL calibrations of CPW transmission lines of different dimensions, we are able to extract the real and imaginary parts of the dielectric permittivity as a function of frequency from 1 to 40 GHz. By performing such measurements under the application of a bias voltage, we are able to determine the relevant dielectric quantities (dielectric loss, tuning, and figure of merit) for dielectric materials of interest for tunable microwave applications. We have demonstrated this technique with measurements of the dielectric properties of a 0.4 µm $Ba_{0.5}Sr_{0.5}TiO_3$ thin film at room temperatures. The ability to perform such measurements as a function of frequency and temperature should be

valuable for the understanding and optimization of tunable thin film materials for microwave applications.

ACKNOWLEDGMENTS

REFERENCES

[1] A.T. Findikoglu, Q.X. Jia, I.H. Campbell, X.D. Wu, D. Reagor, C.B. Mombourquette, and D. McMurry, Appl. Phys. Lett **66**, 3674 (1995).

[2] D.C. DeGroot, J.A. Beall, R.B. Marks, and D.A. Rudman, IEEE Trans. Applied Supercond. **5**, 2272 (1995).

[3] Q.X. Jia, X.D. Wu, S.R. Foltyn, and P. Tiwari, Appl. Phys. Lett. **66**, 2197 (1995).

[4] J.D. Baniecki, R.B. Laibowitz, T.M. Shaw, P.R. Duncombe, D.A. Neumayer, D.E. Kotecki, H. Shen, and Q.Y. Ma, Appl. Phys. Lett. **72**, 498 (1998).

[5] S. Zafar, R.E. Jones, P. Chu, B. White, B. Jiang, D. Taylor, P. Surcher, and S. Gillepsie, Appl. Phys. Lett. **72**, 2820 (1998).

[6] H. Chang, I. Takeuchi, and X.-D. Xiang, Appl. Phys. Lett. 74, 1165 (1999).
[7] F.A. Miranda, C.H. Mueller, C.D. Cubbage, K.B. Bhasin, R.K. Singh, S.D. Harkness, IEEE Trans. Appl. Supercond. **5**, 3191 (1995).

[8] W. Chang, J.S. Horowitz, A.C. Carter, J.M. Pond, S.W. Kirchoefer, C.M. Gilmore, and D.B. Chrisey, Appl. Phys. Lett. **74**, 1033 (1999).

[9] R.B. Marks, IEEE Trans. Microwave Theory Tech. **39**, 1205 (1991).

[10] D.F. Williams and R.B. Marks, 38th ARFTG Conf. Digest, pp.68-81, March 1992.

[11] D.F. Williams and R.B. Marks, IEEE Trans. Microwave Guided Wave Lett. **1**, 243 (1991).

[12] D.F. Williams and R.B. Marks, IEEE Trans. Microwave Guided Wave Lett. **1**, 141 (1991).

[13] D.F. Williams and R.B. Marks, IEEE Trans. Microwave Guided Wave Lett. **3**, 247 (1991).

[14] M.D. Janezic and D.F. Williams, IEEE International Microwave Symposium Digest, Vol.**3**, pp. 1343-1345, June, 1997.

[15] E. Carlsson and S. Gevorgian, IEEE Trans. Microwave Theory Tech. **47**, 1544 (1999).